A Theoretical Model Of The Surface Geometry Of Laminar Fluid Chains

Zachary Zitzewitz[1]

1 Personal Section

During the first visit to my friend's house since the pandemic had started, the first thing I did was wash my hands. The first thing I noticed was the eye-catching shape of the water projecting from the faucet. While the sinks I had used for the past year emitted frothy, turbulent jets, the water in this sink fell over a flat edge and created a laminar cascade of water that appeared to take the shape of mutually orthogonal chain links. I decided I had to discover what was going on. When I got home, I scoured the internet and found some qualitative explanations, but not much more. Maybe it was because I had just taken differential geometry at school and a course on planetary-scale ocean dynamics with another educational program, or that I had worked on fluid dynamics simulations for an autonomous underwater robotics project, but I really wanted to devise a mathematical description of this phenomenon. I love understanding not just the intuition behind why things happen, but the equations as well.

I attended a small middle and high school that was tailor-made for kids who love math, and this allowed me to receive a mathematical and scientific education that was both broad and fairly deep. I was already able to take courses on differential equations or Lagrangian mechanics, which gave me much of the necessary background for the problem I was working on. However, I learned most of the content that was specifically related to fluid dynamics, as well as some harder techniques for dealing with partial differential equations, by finding and reading textbooks and papers on my own and occasionally talking about them with my physics teacher.

I went into this project with no real expectations. I initially started by trying to see if I could figure out whether I could actually describe something from the real world, but I became increasingly more invested in the problem. When I finally wrote code to numerically solve the system I had derived and it looked similar to what I had observed, I was ecstatic. I find that abstract mathematics can be beautiful, but mathematics really shines in its power to describe the world that we live in.

Particularly for high schoolers who are interested in math and science research, it is important to remember that your curiosity need not be constrained by the size of the laboratory or other experimental apparatuses that you may or may not have access to. You can ask a question about anything. One of the great things about our world is that it can be modeled by mathematics, and one of the great things about mathematics is that it can be done anywhere. But because math is a gargantuan field, not all of it will be relevant to your specific topic. In my opinion, the hardest part is figuring out which tools will be helpful and

[1]Proof School (zacharyzitzewitz@proofschool.org). I would like to thank Kaushik Basu for his advice throughout the process.

which will not. Having a broad exposure to various subfields can help with this problem, as well as give new ways of thinking about it, and there are so many well-explained resources on the internet that can both give you a foundation in a new discipline or simply fill in the gaps. Finally, it is important to actually have an interest in your topic. For me, it was fluid dynamics, but it really can be anything!

2 Introduction

I present a theoretical model of gravity-driven laminar fluid chains. A stream of fluid falls under this categorization based on the distinctive shape of its mutually orthogonal sheets of fluid bounded by curved jets, which will be referred to throughout this discussion as “chain links.” If the fluid falls through specific orifice geometries under the influence of gravity, the chain will be oriented downwards. The jets that bound the sheets collide over and over again, pulled towards each other by surface tension and cascading down through the system. This paper will present both a qualitative explanation of this phenomenon and simulation of it based on a mathematical model. The figure below shows an example of one such chain link.

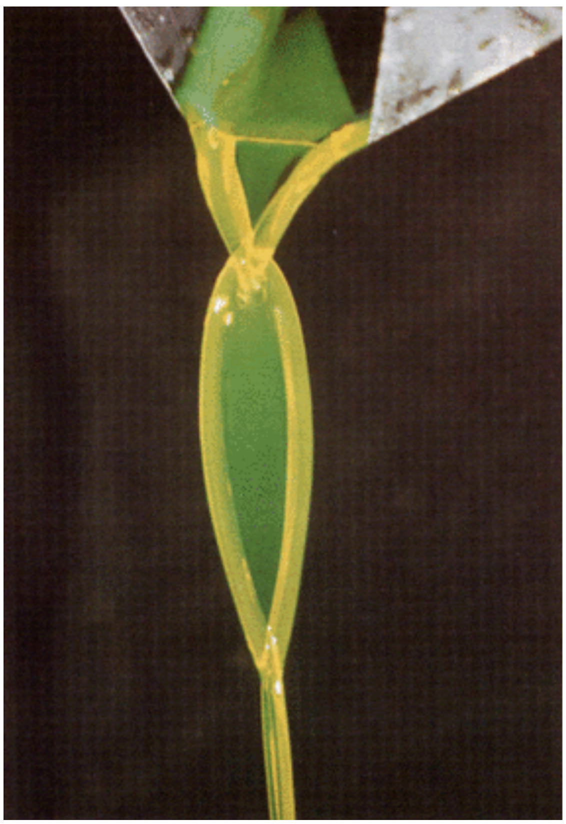

Credit for the image goes to Johnson et al. [1], who were able to seed the fluid with fluorescein and illuminate it with ultraviolet light for extra visibility.

For the purposes of this paper, the flow within the sheet and jets will both be treated as laminar. The analysis will consider the case with no motion of the fluid in directions perpendicular to the direction of flow, nor eddies, vortices, or turbulence of any other kind in the stream.

Laminar fluid chains appear naturally in multiple places. Common examples are when liquids are poured from a pitcher or fall from a waterspout. They have been recorded as early as 1879, by Lord Rayleigh [2]. Investigations into the instability of these chains and the "fishbone"-like structure that appears under a strobe light were undertaken by Bush and Hasha [3]. Their chain structure was obtained by colliding two identical laminar jets at an angle, rather than pouring the liquid off of a ledge. This creates a more pronounced and adjustable liquid sheet, which has several applications including electron spectroscopy at the nanometer scale [4] and fuel injection in liquid rocket motors [5].

The fluid chains were also simulated by Sanjay and Das [6], who used a three-dimensional finite volume framework to obtain time-dependent solutions to the Navier-Stokes equations. This method is computationally expensive because the modeling of the moving interface between the air and water involves interface construction, geometric flux computation, and interface advection, all complicated steps. By assuming that the chain is already in a steady state, I propose a model that relies on a much simpler system of only four first-order differential equations that can be derived from basic principles of physics.

3 Intuition

The main reason for the distinctive shape of the mutually orthogonal chain links can be explained by a simple argument involving surface tension and inertia [7]. A cross-sectional slice of the chain in the xy-plane assumes a long and narrow shape with width w and larger circles of radius R at each endpoint. As the surface area of the air-water interface is proportional to the energy associated with surface tension, the laminar flow seeks to minimize this surface area and hence contracts inwards towards a circular shape. However, the water still has inertia and thus overshoots this circular shape, directing the water in a similarly-shaped cross-section oriented orthogonally to the original. This oscillation of the cross-section with respect to the z-axis explains why the laminar flow takes the form of a chain. The evolution of the cross-section of the fluid chain along this axis is depicted below. The three curves show the boundary of the fluid for each value of z, highlighted on the image below.

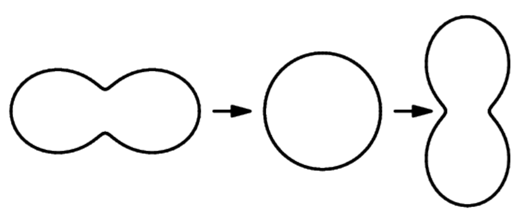

The author generated this particular chain by pouring distilled water out of a pitcher. Dye was added for increased visibility, but had no measurable effect on surface tension and density.

The amplitude and spatial period of each link of the chain diminishes with distance, which can be explained by viscous dissipation. The force due to viscosity is proportional to the normal velocity gradient. Thus, the velocity gradient exponentially approaches 0, in which case the water does not move in the plane perpendicular to the z-axis. In order for this to happen, the forces from surface tension must completely cancel out. Thus, the jet eventually assumes a circular cross-section.

Another shape that the laminar fluid flow can take is that of a double helix, with one continuous sheet bounded by the same two jets as they twist around the surface. The chain may become a helix under slightly different initial conditions, with the jets having velocities perpendicular to both the z axis and the vector from the center of the jet to the center of the helix. If the force from surface tension and pressure gradient in the water exactly induces the acceleration due to uniform circular motion about the axis of the helix, then the jets on either side will assume a spiral geometry rather than that of a chain.

4 Mathematical Model

Given a laminar fluid chain, it may be broken up into several links, as shown below:

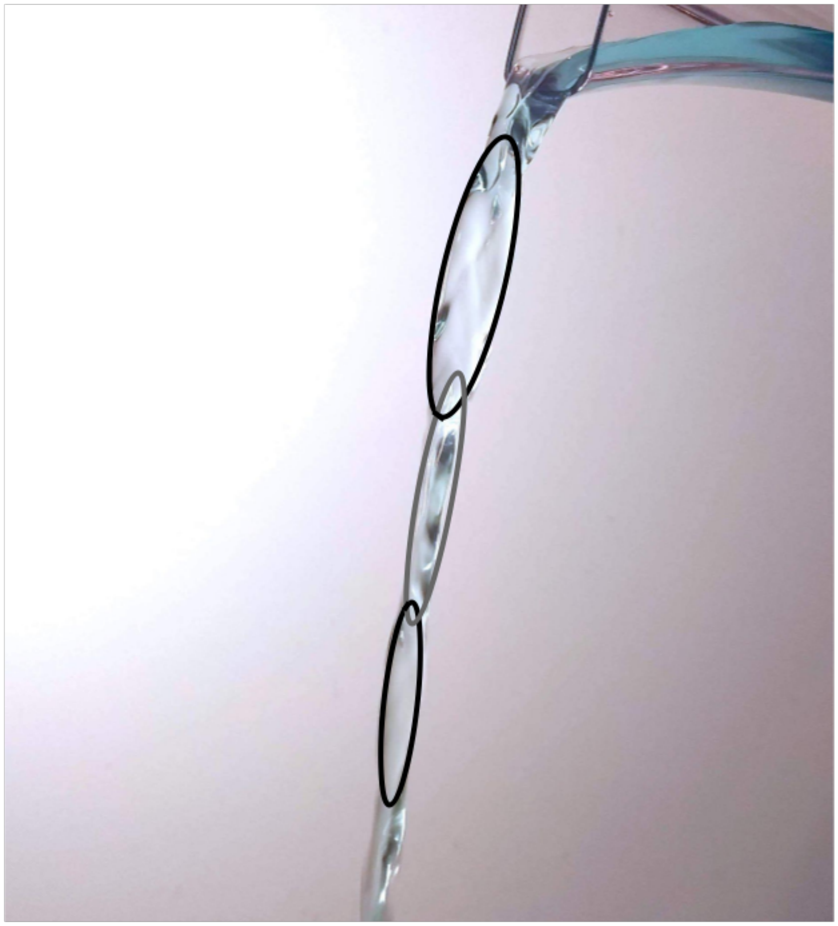

We can model each link of the laminar fluid chain as a symmetric pair of curved laminar jets of water connected by a thin sheet of water. The breaking up of the chain link into these three parts is similar to Kashnaj and Kebriaee's treatment [5], expect without the jet misalignment. The jets originate from the origin and are centered along the curve $\vec{\gamma}$, which may be expressed in polar coordinates as $(\gamma(\theta); \theta)$. The arc length s of $\vec{\gamma}$ is thus

$$s(\theta) = \int_0^\theta ds = \int_0^\theta \sqrt{\gamma^2 + \left(\frac{d\gamma}{d\theta}\right)^2} d\theta.$$

Furthermore, $\vec{\gamma}$ has curvature

$$\kappa = 1/R = \left|\left|\frac{d^2\vec{\gamma}}{ds^2}\right|\right|.$$

The jets themselves may be characterized as circular tubes of radius r, a function that varies with s and thus θ.

The thin sheet of water may be characterized by its width w at every point. The water in the jet has speed v along $\frac{d\vec{\gamma}}{d\theta}$, and the water in the sheet has speed u radially away from the origin. We make the simplifying assumption that the speed u is constant everywhere in the sheet, as justified by Taylor [7]. A depiction of how γ and the associated variables are oriented is below:

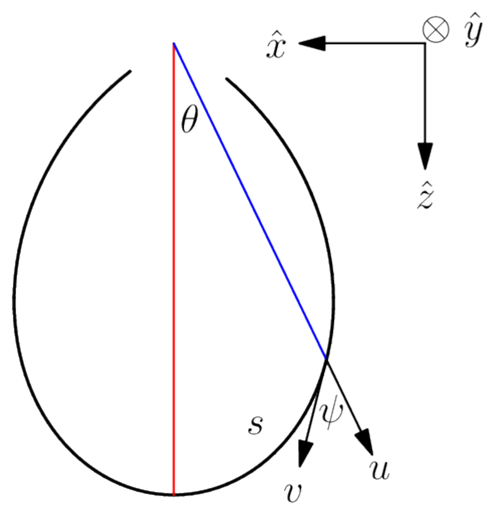

θ is defined to be the angle measured from the z-axis in the negative direction. ψ is defined to be the angle between the vectors $\vec{\gamma}$ and $\frac{d\vec{\gamma}}{d\theta}$ for later convenience. These variables completely characterize the surface of the chain. Dividing it into the jets and the sheet, we can parametrize the surface in three dimensions like so. (The parameters satisfy the bounds $-\frac{\pi}{2} \leq \theta \leq \frac{\pi}{2}$, $-\pi \leq \phi \leq \pi$, and $0 \leq d \leq 1$.)

$$\Sigma_{\text{jet}}(\theta, \phi) = \begin{bmatrix} \gamma(\theta)\cos\theta + \frac{\partial \gamma}{\partial z} r(\theta)\cos\phi \\ r(\theta)\sin\phi \\ \gamma(\theta)\sin\theta - \frac{\partial \gamma}{\partial x} r(\theta)\cos\phi \end{bmatrix} \tag{1}$$

$$\Sigma_{\text{sheet}}(d, \theta) = \begin{bmatrix} d\gamma(\theta)\cos\theta \\ \pm w \\ d\gamma(\theta)\sin\theta \end{bmatrix} \tag{2}$$

The following identities, which will prove to be useful later, may be derived from basic geometry:

$$ds^2 = d\gamma^2 + \gamma^2 d\theta^2 \quad \text{and} \quad \sin\psi d\gamma = \cos\psi\gamma d\theta. \tag{3}$$

The parameters of the water and surrounding environment are also important for determining the geometry of the laminar fluid chain. They are

- the density $\rho = 1.0 \times 10^3$ kg/m^3, with dimensions [ML^{-3}]
- the surface tension $\sigma = 7.2 \times 10^{-2}$ N/m, with dimensions [MT^{-2}]
- the dynamic viscosity $\mu = 7.9 \times 10^{-4}$ Pa $\cdot$ s, with dimensions [ML^{-1}T^{-1}]
- the acceleration due to gravity $g = 9.8$ m/s^2, with dimensions [LT^{-2}]

Keeping track of dimensions is useful when confirming the validity of fluid dynamics equations.

4.1 Force Balancing

Consider a section of the fluid chain between θ and $\theta + d\theta$. It may be approximated by a small sector of a torus with outer radius $R = 1/\kappa$ and inner radius r. At the point $\vec{\gamma}(\theta)$, we may use the system of coordinates with $\hat{n}$ oriented perpendicular to $\vec{\gamma}$, pointing outward; $\hat{t}$ pointing along $\frac{d\vec{\gamma}}{d\theta}$; and $\hat{b}$ pointing directly into the plane of the sheet. The coordinate system $\{\hat{n}, \hat{t}, \hat{b}\}$ is both right-handed and orthonormal. We will consider the components of the forces acting in the directions normal ($\hat{n}$) and tangential ($\hat{t}$) to the curve independently. A free body diagram describing all of the important forces is below. Note that the forces are not drawn to scale for readability.

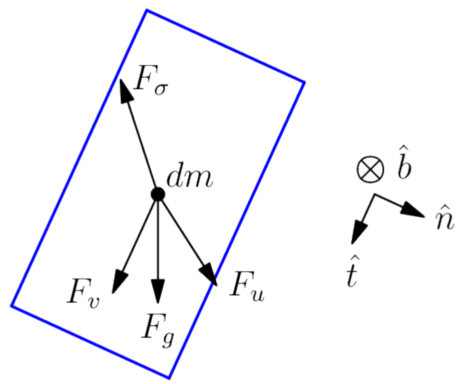

4.2 Normal Component

We first consider the normal component of each force and reconcile this with Newton's laws to produce a partial differential equation:

- The mass and acceleration experienced by the fluid as a result of moving along the curved path $\vec{\gamma}$ is

$$ma = -\frac{mv^2}{R}\hat{n} = \kappa v^2(\rho\pi r^2 R)d\theta\ \hat{n} = \pi\rho v^2 r^2 d\theta\ \hat{n}.$$

- The force acting on the sector due to the momentum flux from the water sheet is

$$F_u = u\frac{dm}{dt} = \rho w R(u^2 \sin^2\psi)d\theta\ \hat{n}.$$

- The force acting on the sector due to gravity is simply

$$F_g = -mg\hat{z}_\perp = \rho g\pi r^2 R\sin(\psi - \theta)d\theta\ \hat{n}.$$

- The force acting on the sector due to surface tension is more complicated and can be derived from the Young-Laplace equation [8], which relates the difference in pressure $\Delta P = \sigma(\nabla \cdot \hat{\xi})$ across the air-water interface. Here, $\hat{\xi}$ is the unit vector normal to the surface Σ. However, it has been shown that the divergence of the surface normal $\nabla \cdot \hat{\xi}$ is simply equal to the sum of the principal curvatures κ_1 and κ_2 of the surface at every point [9]. If we approximate the surface of the jet to be a small slice of a torus, its parametrization is

$$\Sigma_{\text{torus}}(\theta, \phi) = \begin{bmatrix} (R + r\cos\phi)\cos\theta \\ (R + r\cos\phi)\sin\theta \\ r\sin\phi \end{bmatrix},$$

and its principal curvatures are

$$\kappa_\phi = -\frac{1}{r} \text{ and } \kappa_\theta = -\frac{\cos\phi}{R + r\cos\phi}.$$

Intuitively, this should make sense: the radius of curvature in the ϕ direction is just the distance r because it is always perpendicular to the normal, while the radius of curvature in the θ direction depends on both the distance to the axis of the torus and which direction the normal vector is pointing. This may be seen in the figure below, where the osculating circles have radii r and $\frac{R+r\cos\phi}{\cos\phi}$.

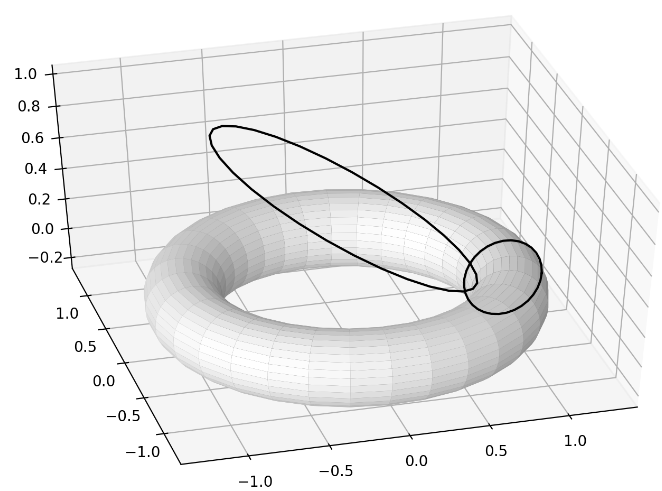

Finally, before performing the surface integral, we need an expression for the infinitesimal surface normal element $d\vec{S}$. It is approximately a rectangle with width $(R + r\cos\phi)d\theta$ and height $rd\phi$, oriented in the direction $\cos\phi\,\hat{n} + \sin\phi\,\hat{b}$. However, because we are only concerned with the forces in the $\hat{n}$-direction and the chains are symmetric along the $\hat{b}$-axis, we may disregard the $\sin\phi\,\hat{b}$ term. Integrating over the whole surface yields the net force due to surface tension

$$\begin{aligned}
F_\sigma &= \iint_\Sigma \sigma(\nabla \cdot \hat{\xi}) d\vec{S} \\
&= \iint_\Sigma \sigma(\kappa_\theta + \kappa_\phi) d\vec{S} \\
&= -\sigma \int_0^{2\pi} \frac{R + 2r\cos\phi}{r(R + r\cos\phi)} \cdot r(R + r\cos\phi)\cos\phi \hat{n} \cdot d\phi d\theta \\
&= -2\sigma\pi r d\theta\ \hat{n}.
\end{aligned}$$

Now that we have the $\hat{n}$ components of each force, we apply Newton's second law. The sum of the forces on the sector yields the equation

$$\begin{aligned}
ma &= F_u + F_g + F_\sigma \\
\implies 0 &= \pi\rho v^2 r^2 \kappa + \rho w u^2 \sin^2\psi + \rho g \pi r^2 \sin(\psi - \theta) - 2\sigma\pi r\kappa. \qquad (4)
\end{aligned}$$

4.3 Tangential Component

We next consider the the tangential component of each force to produce a similar equation to the one above:

- The tangential momentum flux within the boundary jet is

$$F_v = \frac{\partial}{\partial s}(\pi\rho v^2 r^2) R d\theta\ \hat{t}.$$

- The force due to the momentum flux from the water sheet is

$$F_u = u\frac{dm}{dt} = -(u^2 \sin\psi\cos\psi)\rho w R d\theta\ \hat{t}.$$

- The force acting on the sector due to gravity is simply

$$F_g = -mg\hat{z}_\parallel = \rho g \pi r^2 \gamma \cos(\psi - \theta) d\theta\ \hat{t}.$$

- The pressure due to the curvature of the boundary again comes from the Young-Laplace equation, but in this case the average value $\langle \nabla \cdot \hat{\xi} \rangle$ is approximately $\frac{1}{R}$. Thus, the force is

$$F_\sigma = \pi r^2 \frac{\partial}{\partial s}\left(\frac{\sigma}{r}\right) \cdot R d\theta\ \hat{t}.$$

- The viscous forces on the sector can be calculated directly from the Navier-Stokes equations [10]:

$$\frac{\partial \vec{u}}{\partial t} + (\nabla \cdot \vec{u})\vec{u} - \nu\nabla^2\vec{u} = -\frac{1}{\rho}\nabla P$$
$$\nabla \cdot \vec{u} = 0.$$

Because the sector is infinitesimally small, we make the following assumptions: the flow is steady, axisymmetric, directed only tangentially to $\vec{\gamma}$, and satisfies continuity. Letting q be the distance from the axis of the flow and v be the tangential velocity of the fluid, the following equation is satisfied:

$$\frac{1}{q}\frac{\partial}{\partial q}\left(q\frac{\partial v}{\partial q}\right) = \frac{1}{\mu}\frac{dP}{ds}.$$

Note that the solution to this equation for a very long cylindrical pipe happens to be equivalent to the Hagen-Poiseuille equation [11]. This allows us to solve for the difference in pressure across a small distance $dx = Rd\theta$. However, the shear velocity $\frac{\partial v}{\partial q}$ is assumed to be 0 within the laminar region of the tube because v is only a function of θ. The velocity throughout a cross-section of the jet perpendicular to $\hat{t}$ is assumed to be constant. Thus, we assume that the effects due to viscosity are negligible.

$$F_\mu = 0.$$

Now that we have the $\hat{t}$ components of each force, we apply Newton's second law. The sum of the forces on the sector yields the equation

$$\begin{aligned} & 0 = F_v + F_u + F_\sigma + F_g \\ \implies & 0 = \frac{\partial}{\partial s}(\pi\rho v^2 r^2) - \rho w u^2 \sin\psi\cos\psi - \rho g \pi r^2 \cos(\psi-\theta) + \pi r^2 \frac{\partial}{\partial s}\left(\frac{\sigma}{r}\right). \end{aligned} \tag{5}$$

4.4 Continuity Argument

We may deduce another equation using the conservation of mass/volume. Because water is incompressible, the volume of water entering per unit time via the fluid sheet is equal to the change in volume of water across the length of the tube, or the tangential gradient of volume flux. Hence,

$$wu\sin\psi = \frac{\partial}{\partial s}(\pi r^2 v). \tag{6}$$

4.5 Putting It Together

In order to actually describe the surface geometry of the chain link, we need to combine these equations into one system of differential equations and solve it. Towards that end, we first rewrite them entirely in terms of the functions $v(\theta)$, $r(\theta)$, $\psi(\theta)$, and $\gamma(\theta)$.

Combining the results from (3), we have

$$ds = \gamma d\theta\sqrt{1+\cot^2\psi} = \gamma\csc\psi d\theta, \quad \text{so} \quad \frac{d}{ds} = \frac{\sin\psi}{\gamma}\frac{d}{d\theta}.$$

Using more geometry and the formula immediately above, we have

$$\kappa = \frac{d}{ds}(\psi+\theta) = \frac{d\psi}{ds} + \frac{d\theta}{ds} = \frac{\sin\psi}{\gamma}\left(1+\frac{d\psi}{d\theta}\right).$$

Finally, we can derive a simple expression for the width of the fluid sheet. Writing the distribution of flux through the sheet as a function of θ as $Q(\theta)$, conservation of volume requires that the width of the sheet w is inversely proportional to the distance from the origin γ. Thus,

$$w = \frac{Q}{u\gamma}.$$

With these identities, we may rewrite the old equations (which had partial derivatives with respect to s) entirely in terms of their derivatives with respect to θ instead, expressed as $v'(\theta)$, $r'(\theta)$, $\gamma'(\theta)$, and $\psi'(\theta)$. The simplified system of equations is given by

$$v' = \frac{2Qu\cos\psi - 2Qv - \frac{Q\sigma}{\rho\pi v r} + 2g\gamma r^2\left(\frac{\cos(\psi-\theta)}{\sin\psi}\right)}{\pi\left(2v^2 r - \frac{\sigma}{\rho}\right)} \cdot \frac{v}{r} \tag{7}$$

$$r' = -\frac{Qu\cos\psi - Qv - \frac{Q\sigma}{2\rho\pi v r} + g\gamma r^2\left(\frac{\cos(\psi-\theta)}{\sin\psi}\right)}{\pi\left(2v^2 r - \frac{\sigma}{\rho}\right)} + \frac{Q}{2\pi v r} \tag{8}$$

$$\psi' = \frac{Qu\sin\psi + g\gamma\pi r^2\left(\frac{\sin(\psi-\theta)}{\sin\psi}\right)}{\pi r\left(\frac{2\sigma}{\rho} - v^2 r\right)} - 1 \tag{9}$$

$$\gamma' = \gamma\cot\psi. \tag{10}$$

The mathematical details behind how these equations were obtained are in Appendix A.

5 Simulation Results

The system of differential equations from the above section was solved numerically, using Euler's Method [12] to simultaneously integrate the functions v, R, ψ, and γ from 0 to $\pi/2$. The surface of the fluid chain is well-approximated by the numerical solutions for small values of θ, but diverge as θ extends beyond $\pm\pi/3$. The final surface generated by this model is shown below:

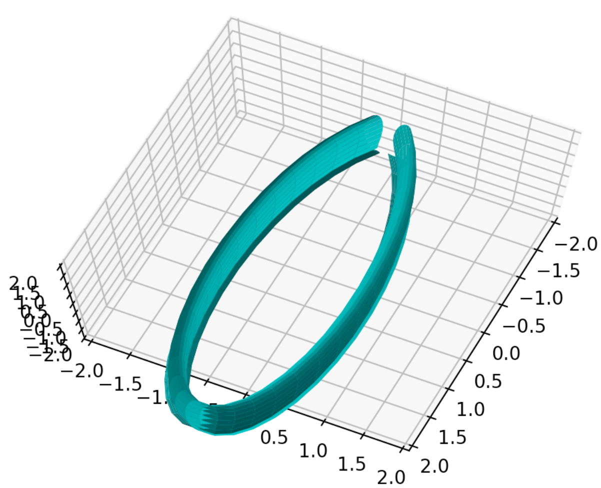

Note that only the bounding jets and not the laminar sheet are included for greater transparency into the structure. The scale is in centimeters.

The flux profile Q as a function of θ was calculated by Sanjay and Das [6] to be an approximately Cauchy distribution with maximum value $Q(0)/Q = 0.6$. This is critical, as a simple zeroth or first order approximation is insufficient. This finding was used along with the initial conditions $\gamma(0)$, the length of the chain link; $r(0)$, the final width of the jets; $v(0) = u$, the velocity of the jets; and $\psi(0) = \pi/2$. Individually changing each of these initial conditions, as well as parameters like density, surface tension, and acceleration due to gravity, changes the geometry in the following ways. Increases in sheet/rim velocity lead to wider chain links. Increases in surface tension lead to wider chain links. Increases in density lead to narrower chain links. Increases in gravitational acceleration led to narrower the links as well, but the effect was only noticeable for $g \gg 10\text{m/s}^2$. In future iterations of this problem, the gravity term is likely not necessary.

6 Conclusion

From this investigation into the geometry of fluid chains, I conclude that this method yields solutions consistent with physical intuition. By dividing laminar streams into infinitesimal fluid elements and considering the individual forces acting on them, equations for the whole surface can be derived. The free surfaces of fluids can be modeled without resorting to computationally expensive techniques for resolving the boundary conditions. Surface tension calculations in particular become drastically simplified by this first-order approximation. This advantage may be helpful when investigating similar problems using this method.

A Explicit Simplification of the System

We begin by simplifying equation (4).

$$
\begin{aligned}
0 &= \pi\rho v^2 r^2 \kappa + \rho w u^2 \sin^2\psi + \rho g \pi r^2 \sin(\psi - \theta) - 2\sigma\pi r\kappa \\
&= \pi\rho v^2 r^2 (1 + \psi') \cdot \frac{\sin\psi}{\gamma} + \rho Q u \sin\psi \cdot \frac{\sin\psi}{\gamma} + \rho g \pi r^2 \sin(\psi - \theta) - 2\sigma\pi r (1 + \psi') \cdot \frac{\sin\psi}{\gamma} \\
&= \rho Q u \sin\psi + \rho g \pi r^2 \gamma \frac{\sin(\psi - \theta)}{\sin\psi} + (\pi\rho v^2 r^2 - 2\pi\sigma r)(1 + \psi') \\
\psi' &= \frac{Q u \sin\psi + g\pi r^2 \gamma \left(\frac{\sin(\psi-\theta)}{\sin\psi}\right)}{\pi r (2\sigma - v^2 r)} - 1
\end{aligned}
$$

Next, we simplify equation (5).

$$\begin{aligned}
0 &= \frac{\partial}{\partial s}(\pi\rho v^2 r^2) - \rho w u^2 \sin\psi\cos\psi - \rho g \pi r^2 \cos(\psi-\theta) + \pi r^2 \frac{\partial}{\partial s}\left(\frac{\sigma}{r}\right) \\
&= \pi\rho(2v^2 r r' + 2 v r^2 v') \cdot \frac{\sin\psi}{\gamma} - \rho Q u \cos\psi \cdot \frac{\sin\psi}{\gamma} - \rho g \pi r^2 \cos(\psi-\theta) + \sigma\pi r' \cdot \frac{\sin\psi}{\gamma} \\
&= 2\pi\rho v r(v r' + r v') - \rho Q u\cos\psi - \rho g \pi r^2 \gamma \frac{\cos(\psi-\theta)}{\sin\psi} + \sigma\pi r' \\
v' &= \frac{Qu\cos\psi}{2\pi v r^2} + \frac{g\gamma\cos(\psi-\theta)}{2\pi v\sin\psi} - \left(\frac{v}{r} + \frac{\sigma}{2\rho v r^2}\right) r'
\end{aligned}$$

Now we simplify equation (6).

$$\begin{aligned}
0 &= wu\sin\psi - \frac{\partial}{\partial s}(\pi r^2 v) \\
&= Q \cdot \frac{\sin\psi}{\gamma} - \frac{d}{d\theta}(\pi r^2 v) \cdot \frac{\sin\psi}{\gamma} \\
Q &= (2\pi r v) r' + (\pi r^2) v'
\end{aligned}$$

We now rewrite these equations to gain explicit values for r' and v' expressed purely in terms of the functions themselves and not their derivatives. This gives us our system of ordinary differential equations:

$$\begin{aligned}
v' &= \frac{2Qu\cos\psi - 2Qv - \frac{Q\sigma}{\rho\pi v r} + 2g\gamma r^2\left(\frac{\cos(\psi-\theta)}{\sin\psi}\right)}{\pi\left(2v^2 r - \frac{\sigma}{\rho}\right)} \cdot \frac{v}{r} \\
r' &= -\frac{Qu\cos\psi - Qv - \frac{Q\sigma}{2\rho\pi v r} + g\gamma r^2\left(\frac{\cos(\psi-\theta)}{\sin\psi}\right)}{\pi\left(2v^2 r - \frac{\sigma}{\rho}\right)} + \frac{Q}{2\pi v r} \\
\psi' &= \frac{Qu\sin\psi + g\gamma\pi r^2\left(\frac{\sin(\psi-\theta)}{\sin\psi}\right)}{\pi r\left(\frac{2\sigma}{\rho} - v^2 r\right)} - 1 \\
\gamma' &= \gamma\cot\psi.
\end{aligned}$$

References

[1] R. Schluter S. Bankoff M. Johnson, M. Miksis. Fluid chains produced by obliquely intersecting viscous jets connected by a thin free liquid film. *Physics of Fluids*, 8(S2), 1996.

[2] Rayleigh. On the capillary phenomena of jets. *Proceedings of the Royal Society of London*, 29, 1879.

[3] John W. M. Bush and Alexander E. Hasha. On the collision of laminar jets: fluid chains and fishbones. *Journal of Fluid Mechanics*, 511, 2004.

[4] et. al Petr Brůža, Chandra B. Curry. Generation and characterization of ultrathin free-flowing liquid sheets. *Nature Communications*, 9, 2018.

[5] S. Kashanj and A. Kebriaee. The effects of different jet velocities and axial misalignment on the liquid sheet of two colliding jets. *Chemical Engineering Science*, 206, 2019.

[6] Vastal Sanjay and Arup Kumar Das. Formation of liquid chain by collision of two laminar jets. *Physics of Fluids*, 29, 2017.

[7] Sir Geoffrey Taylor. Formation of thin flat sheets of water. *Proceedings of the Royal Society of London*, 251, 1961.

[8] Leiv Magne Siqveland and Svein M. Skjæveland. Derivations of the young-laplace equation. *Capillarity*, 4(2), 2021.

[9] Patience Henson. A proof that the divergence of a surface normal is equal to the sum of the principal curvatures. `https://willson.cm.utexas.edu/Research/Sub_Files/Surface_Phenomena/Spring%202000/surface_normal_proof.pdf`.

[10] Doug McLean. *Understanding Aerodynamics: Arguing from the Real Physics*. Wiley, 2012.

[11] S P Sutera and R Skalak. The history of poiseuille's law. *Annual Review of Fluid Mechanics*, 25, 1993.

[12] Leonhard Euler. *Institutiones calculi integralis*. Lipsiae Et Berolini, 1768.